Energy and angular distributions of Z^0-production at LEP/LHC energies

A. Gutiérrez-Rodríguez and A. Rosado
Instituto de Física, Universidad Autónoma de Puebla.
Apartado postal J-48, Col. San Manuel, 72570 Puebla, Pue., Mexico

Recibido el 4 de julio de 1997; aceptado el 23 de octubre de 1997

We discuss the energy spectrum and angular distributions of Z^0-production in the process $e^- + P \to e^- + Z^0 + X$ in the context of the standard model SU(3)$_C\otimes$ SU (2)$_L\otimes$ U(1) of the strong and electroweak interactions at LEP/LHC energies. We find that these distributions are strongly peaked, which means that the Z^0-bosons will be mainly produced in a small, well determined region of phase space.

Keywords: Heavy boson production, *ep* collisions

Discutimos el espectro de energía y las distribuciones angulares de la producción de Z^0 en el proceso $e^- + P \to e^- + Z^0 + X$ en el contexto del modelo estandard SU(3)$_C\otimes$ SU (2)$_L\otimes$ U(1) de interacciones electro débiles y fuertes en las energías LEP/LHC. Se encuentra que esas distribuciones son muy picudas, lo que significa que los bosones Z^0 serán producidos en una región pequeña pero bien definida del espacio fase.

Descriptores: Producción de bosones, colisiones *ep*

PACS: 14.70.Hp; 13.60.Hb; 13.85.Qk

1. Introduction

LEP/LHC will provide us with the possibility to observe ep-collisions with a maximal energy $E^{\max} = 60$ GeV of the electron and $E_p^{max} = 7$ TeV of the proton [1]. Even that at LEP I has been already measured with high precision most of the Z^0 boson properties, one of the interesting experiments at LEP/LHC will be electroproduction of weak bosons because that would be a way to test the different parton distribution functions which exist in the literature. In the case of the neutral gauge boson Z^0, its decays to lepton pairs will provide a clear signal of its production. Neutral bosons can be produced through neutral current and charged current interactions. The production rate for neutral current processes is bigger than that for charged current processes, because in the latter case photon-exchange diagrams do not contribute in the lowest order of α. Moreover the production of a Z^0 in ep-scattering in the case of the neutral current process with an electron in the final state is easier to detect than that in the charged current process with a neutrino in the final state. Therefore we discuss in this work Z^0-production in the deep inelastic process

$$e^- + p \to e^- + Z^0 + X, \tag{1}$$

using the standard model SU(3)$_C\otimes$ SU(2)$_L\otimes$ U(1) of the strong and electroweak interactions [2] and the parton model [3] with the parton distribution functions of J. Botts *et al.* [4], which take into account scaling violations and the charm contribution. We will take $M_{Z^0} = 91.2$ GeV for the mass of the Z^0-bosons and $\sin^2\theta_W = 0.223$ for the electroweak mixing angle.

In the lowest order in α two types of reaction mechanisms will contribute: Z^0-production at the leptonic and hadronic vertex. A first estimation of the Z^0-production rates was given by Llewelyn-Smith and Wiik and 1977 [5]. Other author have reported also calculations for this process [6–8].

In this paper our aim is to discuss the energy E_k and angular distribution θ_k, ϕ_k for given x and y, *i.e.* for given energy and polar angle of the scattered electron [9]. Hence we write down explicitly the kinematical limits for the production angle θ_k of the boson Z^0:

$$-1 \leq \cos\theta_k < \frac{(2Ey - E_k)}{\sqrt{E_k^2 - M_Z^2}}, \tag{2}$$

and use it to introduce a parameter r, defined as follows:

$$r = \frac{1+\cos\theta_k}{1 + (2Ey - E_k)/\sqrt{E_k^2 - M_Z^2}}. \tag{3}$$

The differential cross section $d\sigma^{ep}$ for (1) is calculated in the parton model from the cross section $d\sigma^{eq}$ of the parton subprocess $e^- + q \to e^- + q + Z^0$ and the parton distribution functions $f_q(x', \widetilde{Q}^2)$, which are the probabilities to find a parton q with the fraction x' of the nucleon momentum: $q^\mu = x' p_p^\mu$ in a scattering process with momentum transfer square $\widetilde{Q}^2$.

We discuss in another work the dependence of the differential cross section on the dimensionless variables x and y with the aim to compare the production from the leptonic vertex and the hadronic vertex [10].

We will restrict here our discussion of the energy and angular distribution of the Z^0-production to the region which is experimentally easily accesible and where we have a large cross section, *i.e.*, $x > 0.01$ and $y > 0.5$. But there the production from the lepton vertex dominates by far [10] and we can identify the scale parameter as usual, $\widetilde{Q}^2 = Q^{'2} = sx'y'$ and we have

$$d\sigma^{ep} \approx d\sigma^{ep}_{\text{leptonic}} = \sum_q \int dx' f_q(x', Q^{'2}) d\sigma^{eq}_{\text{leptonic}} . \quad (4)$$

The parton distributions can be used only for $Q^{'2}$ not too small. Therefore we need a cutoff for $Q^{'2}$. Furthermore in order to separate deep inelastic from elastic scatteringn a cut on the invariant mass W of the unobserved particles in the final state is required. The cuts for $Q^{'2}$ and W constrain further the physically allowed region for the process (1) as follows:

$$-(p - p' - k)^2 = Q^{'2} = sx'y' \geq Q^{'2}_{\text{cut}},$$
$$(p + p_p - p' - k)^2 = W = sy'(1 - x') \geq W_{\text{cut}} . \quad (5)$$

Note that a cut W_{cut} on the invariant mass W implies a cut on $Q^{'2}$:

$$Q^{'2}_{W_{\text{cut}}} \geq W_{\text{cut}} \frac{x'}{1 - x'} \geq W_{\text{cut}} \frac{x + \mu/y}{1 - (x + \mu/y)}, \quad (6)$$

with $\mu = M_Z^2/s = M_Z^2/4EE_p$.

Taking an energy in the center of mass of 1,296 GeV, $Q^{'2}_{\text{cut}} = Q^2_{\text{cut}} = 4$ GeV and $W_{\text{cut}} = 10$ GeV^2 we get for the total Z^0-production cross section $\sigma^T = 5.8 \times 10^{-37}$ cm^2. These cuts are suited for the parton distribution functions of J. Botts *et al.* [4] which we use in our performances. This total cross section rate leads to a total production of around 290 Z^0 bosons *per annum* for an integrated luminosity of 500 pb^{-1}, which is expected to be reached at LEP/LHC.

Next we present the dependence on x and y of the cross section for $W_{\text{cut}} = 10$ GeV^2 and two differents values of Q^2_{cut}, namely 4 GeV^2 and 10 GeV^2. We show in Fig. 1 our results for ep-scattering at LEP/LHC with an electron energy of $E_e = 60$ GeV and a proton energy $E_p = 7$ TeV. We can observe in Fig. 1 that the cross section increases as x approaches to 0 and y to 1. We also see that the difference between the results for $Q^{'2}_{\text{cut}} = 4$ GeV^2 and $Q^{'2}_{\text{cut}} = 10$ GeV^2 is generally small. It becomes biggest for small x and $y \to 1$, for example we find for $x = 0.1$ and $y = 0.9$ a relative difference of 10%.

Our results for the dependence of the cross section on the energy E_k and the polar angle θ_k of the produced Z^0-boson, $\log_{10}\left[(d\sigma/d\cos\theta_k dE_k dxdy)/(d\sigma/dxdy)\right]$ *vs.* E_k and $r(E_k, \cos\theta_k)$ are presented in Fig. 2 for $x = 0.008$ and $y = 0.95$, taking $Q^{'2}_{\text{cut}} = 4$ GeV^2 and $W_{\text{cut}} = 10$ GeV^2 (for these values of x and y we need to take into account only the contribution from the lepton vertex). We see from this figure that the Z^0-bosons will be mainly produced in a small E_k interval and for $r \approx 1$. The latter means according to the definition of r [Eq. (3)] that the Z^0 will be mainly found in

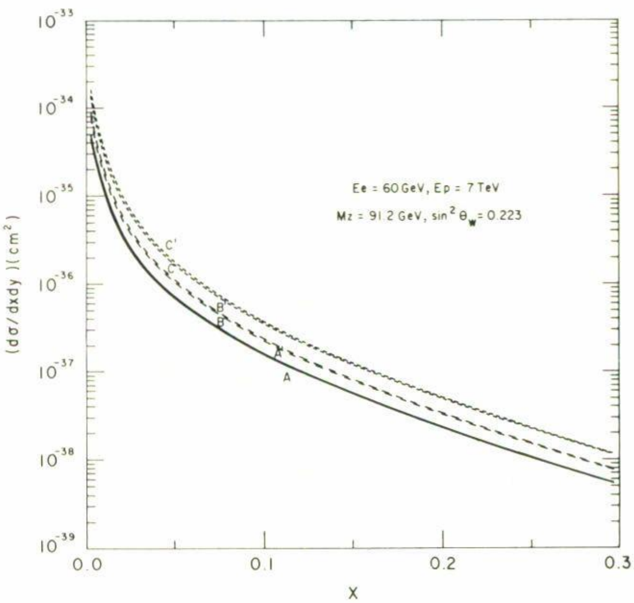

FIGURE 1. $d\sigma/dxdy$ as function of x: for $y = 0.8$ (curve A), $y = 0.9$ (curve B), and $y = 0.95$ (curve C), with $Q^{'2}_{\text{cut}} = 4$ GeV^2; and for $y = 0.8$ (curve A'), $y = 0.9$ (curve B'), and $y = 0.95$ (curve C'), with $Q^{'2}_{\text{cut}} = 10$ GeV^2 ($\sqrt{s} = 1,296$ GeV).

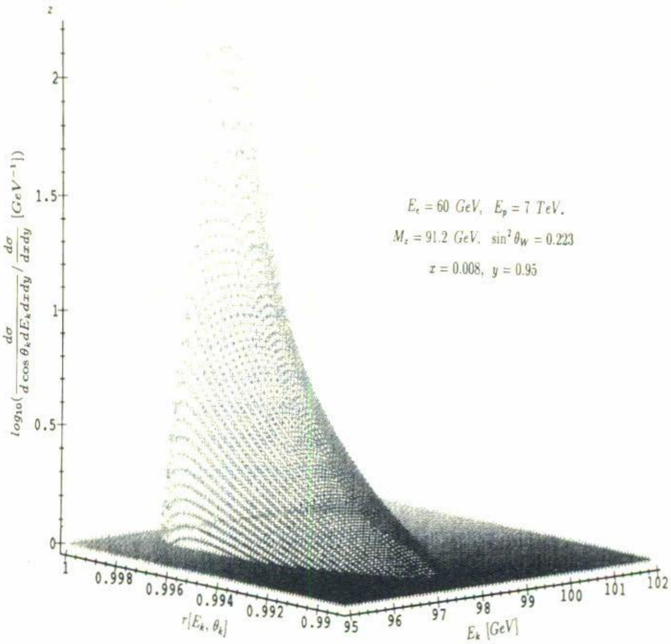

FIGURE 2. Logarithmic plot of the dependence of $d\sigma/dxdy$ on E_k and r for $x = 0.008$ and $y = 0.95$ ($\sqrt{s} = 1,296$ GeV).

the backward direction and that the $\cos\theta_k$ distribution has a sharp peak before it reaches its kinematic upper limit given in (2). We also have observed that most of the Z^0-bosons are produced in the plane which is spanned by the momenta of the incoming and outgoing leptons, *i.e.*, $\sin\phi_k \approx 0$. The reason for these sharp energy and angular distributions is that the diferential cross section becomes large when $Q^{'2} = -(p - p' - k)^2$ approaches its minimal value, $Q^{'2} \approx Q^{'2}_{W_{\text{cut}}}$.

According to the expression given in (6) this happens when $x' \approx x + \mu/y$ and hence $y' \approx (Q'^2/s)/(x + \mu/y) \ll 1$.

These expression for x', y' give for E_k, $\cos\theta_k$ and $\sin\phi_k$:

$$E_k(x, y) \approx Ey + E_p\mu/y + E_p x(1 - y), \quad (7)$$

$$\cos\theta_k(x, y, E_k) \approx (2Ey - E_k)/\sqrt{E_k^2 - M_Z^2}, \quad (8)$$

$$\sin\phi_k \approx 0. \quad (9)$$

These estimates are confirmed by the direct numerical evaluation with a rather good accuracy. This evaluation proved also that the distributions in Fig. 2 are not sensitive to those variations of the cuts which we discussed above. We have included in our computations besides the photon-exchanges also the Z^0-exchange diagrams. As expected, γ-exchange diagrams dominate by far. However, for Q'^2 of order $O(M_Z^2)$ γ-exchange as well as Z^0-exchange are important. From expressions (6) we see that this will happen when $x + \mu/y \approx 1$.

We can summarize our results as follows. If the energy and polar angle of the scattered electron are fixed by given values of the scaling variables x and y, the boson Z^0 will be mostly produced with energy $E_k \approx Ey + E_p x(1 - y) + M_Z^2/(4yE)$, polar angle $\cos\theta_k \approx (2Ey - E_k)/\sqrt{E_k^2 - M_Z^2}$ and azimuthal angle $\sin\phi_k \approx 0$. Due to the number of Z^0 bosons which will be produced at LEP/LHC (290 yearly), it seems to be possible to reconstruct experimentally the narrow kinematic configuration for the Z^0-production.

We end this paper pointing out that the resonance-like behaviour of the E_k and θ_k distributions will help to discriminate between the production of a standard Z^0 and the production of other particles, such as those predicted by other theories with other reaction mechanisms, for example supersymmetry [11] and subconstituent models. [12]

∗. Supported by a CONACyT scholarship and SNI

†. Supported in part by the CONACyT and SNI

1. See, *e.g.*, R. Rückl, preprint MPI-PAE/PTh 76/90 and references therein.
2. S. Weinberg, *Phys. Rev. Lett.* **19** (1967) 1264; A. Salam, *Proc. 8th Nobel Symposium*, edited by N. Svartholm, (Stockholm, 1968), S. 367; S.L. Glashow, J. Illiopoulos, and L. Maiani, *Phys. Rev. D* **2** (1970) 1285.
3. R.P. Feynman, *Photon-Hadron Interactions*, (Benjamin, Reading, Massachusetts, 1972).
4. J. Botts *et al.*, preprint Fermilab-Pub-92/371.
5. C.H. Llewelyn-Smith and B.H. Wiik, *DESY Report* 77/36 (1977).
6. P. Salati and J.C. Wallet, *Z. Phys. C* **16** (1982) 155.
7. G. Altarelli, G. Martinelli, B. Mele, and R. Rückl, *Nucl. Phys.* **B262** (1985) 204.
8. E. Gabrielli, *Mod. Phys. Lett.* **A1** (1986) 465.
9. M. Böhm and A. Rosado, *Z. Phys. C* **34** (1987) 117.
10. A. Gutiérrez-Rodríguez and A. Rosado, (in preparation).
11. H.E. Haber and G.L. Kane, *Phys. Rep.* **117** (1985) 75.
12. See, *e.g.*, R.J. Cashmore *et al*, *Phys. Rep.* **22** (1985) 277 and references therein.